A TIME-DOMAIN PRECONDITIONER FOR THE HELMHOLTZ EQUATION

CHRISTIAAN C. STOLK

ABSTRACT. Time-harmonic solutions to the wave equation can be computed in the frequency or in the time domain. In the frequency domain, one solves a discretized Helmholtz equation, while in the time domain, the periodic solutions to a discretized wave equation are sought, e.g. by simulating for a long time with a time-harmonic forcing term. Disadvantages of the time-domain method are that the solutions are affected by temporal discretization errors and that the spatial discretization cannot be freely chosen, since it is inherited from the time-domain scheme. In this work we address these issues. Given an indefinite linear system satisfying certain properties, a matrix recurrence relation is constructed, such that in the limit the exact discrete solution is obtained. By iterating a large, finite number of times, an approximate solution is obtained, similarly as in a time-domain method for the Helmholtz equation. To improve the convergence, the process is used as a preconditioner for GMRES, and the time-harmonic forcing term is multiplied by a smooth window function. The construction is applied to a compact-stencil finite-difference discretization of the Helmholtz equation, for which previously no time-domain solver was available. Advantages of the resulting solver are the relative simplicity, small memory requirement and reasonable computation times.

1. INTRODUCTION

Time-harmonic solutions to the wave equation can be computed in the frequency or in the time domain. In the frequency domain, a discrete version of the Helmholtz equation is solved. In the time domain, the periodic solutions to a discrete wave equation with time-harmonic forcing term are sought. Frequency domain methods involve less degrees of freedom. However, the indefinite linear systems resulting from discretizing the Helmholtz equation are often difficult to solve. Time-domain methods can be attractive because they require relatively little memory and are easy to implement if a time-domain solver is available. The introduction of [1] contains a recent overview of time-harmonic wave equation solvers.

Time-domain methods are based on the correspondence between Helmholtz and wave equations. In this paper we will use as example the damped wave equation

$$(1) \qquad \frac{1}{c^2}\frac{\partial^2 u}{\partial t^2} + R\frac{\partial u}{\partial t} - \Delta u = f,$$

where $u = u(t,x)$ is the wave field, $f = f(t,x)$ is the forcing term, Δ is the Laplacian, $c(x)$ is the spatially dependent wavespeed, R is a spatially dependent damping coefficient, and x is in some domain Ω with Dirichlet and/or Neumann boundary conditions. Let $u(x,t), f(x,t)$ and $U(x), F(x)$ be related by

$$(2) \qquad u(x,t) = e^{i\omega t}U(x), \qquad \text{and } f(x,t) = e^{i\omega t}F(x).$$

UNIVERSITY OF AMSTERDAM, KORTEWEG-DE VRIES INSTITUTE, POBox 94248, 1090 GE AMSTERDAM, THE NETHERLANDS

E-mail address: C.C.Stolk@uva.nl.

Then u satisfies a wave equation with forcing term f if and only if U satisfies the following Helmholtz equation with forcing term F

$$(3) \qquad\qquad -\Delta U - \frac{\omega^2}{c^2}U + i\omega RU = F.$$

This equation is supplemented with Dirichlet and/or Neumann boundary conditions that carry over from those for (1).

We briefly review some time-domain approaches. The most basic time-domain method is derived from the limiting-amplitude principle. This principle states that solutions $u(x,t)$ to (1) with zero initial conditions and forcing term

$$(4) \qquad\qquad f(x,t) = e^{i\omega t}F(x)$$

satisfy

$$(5) \qquad\qquad u(x,t) = e^{i\omega t}U(x) + O(1), \qquad t \to \infty$$

under certain conditions on the problem, see [4] and references therein. Thus, if $u(x,t)$ is a (numerical) solution to this initial boundary-value problem, and T is some large time, measured in periods, then an approximate solution to the Helmholtz equation is given by

$$(6) \qquad\qquad e^{-i2\pi T}u(x, 2\pi\omega^{-1}T).$$

We will call this the limiting-amplitude approximate solution for time T. A more advanced method is the exact controllability method [5]. In this method the periodicity of the solutions is enforced using optimization. The starting value for the optimization procedure is typically some partially converged limiting-amplitude solution. Recently more insights in and some improvements to this method were obtained [10], and its parallel implementation was studied [9]. In [1] an optimization approach called WaveHoltz was introduced. This method again uses a form of optimization but with a different optimization functional.

An important feature of the methods just described is that they approximate periodic solutions of a given discrete wave equation. This has two consequences that are in general not desirable. First, the results will be negatively affected by both spatial and temporal discretization errors, while solutions to discrete Helmholtz equations only have spatial discretization errors. Secondly, the method is limited to situations in which a time-domain scheme is available, and not (directly) applicable if one only has a discretization of (3) available, or perhaps only a linear system with similar properties.

In this paper, we will address both of these shortcomings by developing a new time-domain solver for discrete Helmholtz equations. In fact the method can be applied to any linear system

$$(7) \qquad\qquad HU = F,$$

where H is a complex $N \times N$ matrix, such that

$$(8) \qquad \text{there is } c > 0 \text{ such that } \operatorname{Re} H + cI \text{ is symmetric positive semidefinite,}$$

and

$$(9) \qquad\qquad \operatorname{Im} H \text{ is symmetric positive semidefinite}$$

In equation (7) F is a vector in $\mathbb{C}^N$ and U is the unknown, also in $\mathbb{C}^N$. We next describe the steps involved in the construction of the new time-domain solver.

First an $N \times N$ system of second order ODE's

$$(10) \qquad\qquad \frac{\partial u^2}{\partial t^2} + Au + B\frac{\partial u}{\partial t} = f$$

and a frequency parameter ω are constructed. We will look for time-harmonic solutions with frequency ω of the system (10). Note that ω is in general *not* the physical frequency parameter used to derive (7). It is a computational parameter, chosen together with the

matrices A and B, and it depends on H in a way to be specified. Time-harmonic functions $u = e^{i\omega t}U$ and $f = e^{i\omega t}F$, with $U, F \in \mathbb{C}^N$, satisfy (10) if and only if

$$(11) \qquad\qquad (-\omega^2 I + i\omega B + A)U = F.$$

Therefore we will choose A, B and ω such that

$$(12) \qquad\qquad H = -\omega^2 I + i\omega B + A.$$

The system (10) plays the role of a semi-discrete wave equation.

Secondly, this system is time-discretized. This is done in such a way that time-harmonic solutions of the discrete-time system are exactly those of the continuous-time system. I.e. if u_n, f_n are related to U, F by $u_n = e^{i\omega n \Delta t}U$ and $f_n = e^{i\omega n \Delta t}F$ then u_n, f_n are solutions to the discrete-time system if and only if U, F satisfy (11). For this purpose we present two modified leapfrog methods.

So by using non-standard finite-difference derivatives, there are no time-discretization errors for the time-harmonic solutions. This is related to ideas from the papers [11, 21] where it was shown that errors in finite-difference discretizations can be analysed precisely in the Fourier domain, and that finite-difference approximations of derivatives can be designed to minimize such errors over some range of wavenumbers. See also [3] for an optimized time-stepping method.

Having a time-discretization of (10) at hand, the third step is to define a map from a right-hand side F in (7) to an approximation for the solution U. For this we follow the idea of equation (6) with one modification, which is the inclusion of a smooth window function in the time-harmonic forcing term.

It is known that the convergence of limiting-amplitude approximate solutions can be slow in some cases, e.g. in case of resonant wave cavities. Therefore we will not use the approximate solution operator directly. Instead we propose to use it as a preconditioner in an iterative solution method for (7), such as GMRES or BiCGSTAB. This is the fourth and last step of our construction. This use as a preconditioner can also be called Krylov acceleration, as the method itself already approximates the true solution. It can be seen as an alternative to the exact controllability and WaveHoltz methods. Because it is used this way, we will call the new approximate solution operator a *time-domain preconditioner*. The above distinction between frequency- and time-domain methods appears no longer satisfactory for this method: It is based on time-domain methodology, but solves a frequency-domain discrete wave equation.

The term time-domain preconditioner was used before in [25]. In that work a related problem was solved, but the resulting method was substantially different, as the Schrödinger equation was used instead of the wave equation and the resulting time-domain scheme was implicit, and not exactly solved.

The behavior of the proposed method will be explained using theory and examples. It is established theoretically under which conditions the new time-discretizations are stable and that the approximate solutions converge to the exact solution of (7) in the limit of large time parameter T. The numerical examples confirm the converge of the approximate solutions and show that Krylov acceleration is indeed useful to accelerate the solution process. Krylov acceleration makes a difference in particular in the case that a resonant low-velocity zone is present. Parameters of the method include the large time parameter T used in the preconditioner, and a parameter for the window function. Results depend weakly on these parameters, i.e. there is a large set of suitable parameter choices.

A few situations that do not fit in the classical time-domain setting, but can be handled with the new solver are as follows. First one can use it with discretizations that have been designed specifically for the Helmholtz equation. For example finite-difference discretizations that minimize dispersion errors such as those from [2] for the 2-D case and [17, 20, 23]

for the 3-D case. Our examples are about this application. One can also imagine situations where the physical time-domain model is complicated to simulate, but reduces to a relatively simple Helmholtz equation in the frequency domain. A third use case is in the context of a multigrid method. In multigrid methods the coarsest level system still has to be solved by another (non-multigrid) method. It is based on the linear system one started with and on the choice of multigrid method. In Helmholtz equations the convergence can be very sensititve to the choice of the coarse level system and it is recommended to use certain prescribed discretizations [19, 17].

However, the usefulness of the method is not restricted to these cases, and some of the ideas could also be incorporated into other time-domain methods.

The contents of the remainder of the paper is as follows. In section 2, the construction of the new solver is described. In section 3 examples of this construction are given in case H results from certain finite-difference discretizations. Section 4 contains the theoretical results. After that, section 5 contains the numerical examples. We conclude the main text with a discussion section. Appendices contains some material on Fourier analysis used in section 4, and some remarks on the compact-stencil finite-difference discretization described in section 3.

2. Methods

In this section we describe in detail the construction of a time-domain preconditioner for a matrix H satisfying (8) and (9). We recall from the introduction that there are three main steps: (i) the definition of a suitable second order system of ODE's of the form (10); (ii) the definition of a suitable time-integration method for this system of ODE's; (iii) the definition of a linear map that produces approximate solutions based on the limiting-amplitude principle. Step (ii), the time-integration method, will be discussed first, since the properties of the time-integration method affect the choice of the system of ODE's (10). Then steps (i) and (iii) and the application of the method as a preconditioner are discussed. Occasionally we will point forward to section 4, where some properties of the time-discretizations and the preconditioner are proven.

2.1. **Frequency-adapted time discretizations of (10).** The leapfrog or basic Verlet method is a standard method to integrate equations of the form (10) in case that $B = 0$. It is obtained, basically, by discretizing the second order time derivative using standard second order finite differences. To allow for nonzero B, the damping term has to be discretized as well. A standard way to do this is with central differences [6, 16, 15]. This yields the equation

$$(13) \qquad \frac{1}{\Delta t^2}\left(u_{n+1} - 2u_n + u_{n-1}\right) + \frac{1}{2\Delta t}B\left(u_{n+1} - u_{n-1}\right) + Au_n = f_n,$$

from which u_{n+1} can be solved. Note that u_n denotes the discrete approximation to $u(n\Delta t)$, and that $u(t) \in \mathbb{C}^N$. This only leads to an explicit method if B is diagonal. To obtain an explicit method in case B is non-diagonal, the damping term can be discretized by backward differences, which yields the equation

$$(14) \qquad \frac{1}{\Delta t^2}\left(u_{n+1} - 2u_n + u_{n-1}\right) + \frac{B}{\Delta t}\left(u_n - u_{n-1}\right) + Au_n = f_n.$$

Since this method is an order less accurate and has stricter CFL conditions it is only proposed for the case that B is non-diagonal, in the other case (13) is preferred.

We will formally define the time-integrators resulting from (13) and (14).

Definition 1. Let

$$(15) \qquad K = \Delta t^2 A \qquad L = \Delta t B \qquad g_n = \Delta t^2 f_n.$$

Central differences damped leapfrog will be defined as the time integrator given by

$$(16) \qquad u_{n+1} = I_{\mathrm{cd}}(u_n, u_{n-1}, f_n) := \left(I + \tfrac{1}{2}L\right)^{-1}\left((2-K)u_n - (I - \tfrac{1}{2}L)u_{n-1} + g_n\right).$$

Backward differences damped leapfrog will be defined as the time integrator given by

$$(17) \qquad u_{n+1} = I_{\mathrm{bd}}(u_n, u_{n-1}, f_n) := (2 - K - L)u_n - (I - L)u_{n-1} + g_n.$$

The stability of these methods is studied in section 4. According to Theorem 1, I_{cd} is stable if

$$(18) \qquad\qquad K \text{ and } L \text{ are positive semidefinite,}$$

and

$$(19) \qquad\qquad 4I - K \text{ is positive definite,}$$

while I_{bd} is stable if (18) is satisfied and

$$(20) \qquad\qquad 4I - K - 2L \text{ is positive definite.}$$

Conditions (19) and (20) lead to CFL bounds. This will be discussed below.

As mentioned in the introduction, we look for discretizations such that the time-harmonic solutions of frequency ω of the discrete-time system are exactly those of the continuous time system (10). Due to discretization errors this is not the case for the integrators I_{cd} and I_{bd}. In the next proposition we will show that the time-harmonic solutions to (10) satisfy recursions of the same form as (13) and (14), but with different choices of A, B. From these recursions modified schemes can derived that have the desired property.

Proposition 1. *Let u_n and f_n be related to $U, F \in \mathbb{C}^N$ by*

$$(21) \qquad\qquad u_n = e^{i\omega n \Delta t}U, \qquad f_n = e^{i\omega n \Delta t}F$$

and let

$$(22) \qquad \alpha = \frac{(\Delta t\,\omega)^2}{2 - 2\cos(\omega \Delta t)} = \frac{(\Delta t\,\omega)^2}{4\sin(\frac{\omega \Delta t}{2})^2}, \qquad and \qquad \beta = \frac{\omega \Delta t}{\sin(\omega \Delta t)}.$$

Then U, F satisfy (11) if and only if u_n, f_n satisfy

$$(23) \qquad \frac{1}{\Delta t^2}\left(u_{n+1} - 2u_n + u_{n-1}\right) + \frac{1}{2\Delta t}\tilde{B}\left(u_{n+1} - u_{n-1}\right) + \tilde{A}u_n = \alpha^{-1}f_n,$$

where

$$(24) \qquad\qquad \tilde{A} = \alpha^{-1}A, \qquad and \qquad \tilde{B} = \alpha^{-1}\beta B,$$

and if and only if u_n and f_n satisfy

$$(25) \qquad \frac{1}{\Delta t^2}\left(u_{n+1} - 2u_n + u_{n-1}\right) + \frac{\hat{B}}{\Delta t}\left(u_n - u_{n-1}\right) + \hat{A}u_n = \alpha^{-1}f_n,$$

where

$$(26) \qquad \hat{A} = \alpha^{-1}A - \frac{\beta(1 - \cos(\omega \Delta t))}{\alpha \Delta t}B, \qquad and \qquad \hat{B} = \alpha^{-1}\beta B.$$

Proof. To prove the first claim, $\tilde{A}$, $\tilde{B}$ and $\tilde{c}$ will be constructed such that

$$(27) \qquad \frac{1}{\Delta t^2}\left(u_{n+1} - 2u_n + u_{n-1}\right) + \frac{1}{2\Delta t}\tilde{B}\left(u_{n+1} - u_{n-1}\right) + \tilde{A}u_n = \tilde{c}f_n,$$

if and only if (11). Inserting $u_n = Ue^{in\omega\Delta t}$ into (27), results in

$$(28) \qquad \left[\frac{2\cos(\omega \Delta t) - 2}{\Delta t^2} + \frac{i\,\sin(\Delta t\omega)}{\Delta t}B + \tilde{A}\right]Ue^{in\omega\Delta t} = \tilde{c}e^{in\omega\Delta t}F.$$

Using the definitions of α and β to rewrite the left-hand side, this is equivalent to

$$(29) \qquad \left[-\frac{\omega^2}{\alpha} + i\frac{\omega}{\beta}\tilde{B} + \tilde{A}\right] U = \tilde{c}F.$$

Multiplying by α results in

$$(30) \qquad \left[-\omega^2 + i\omega\frac{\alpha}{\beta}\tilde{B} + \alpha\tilde{A}\right] U = \alpha\tilde{c}F.$$

This is equivalent to (11) if $\tilde{c} = \alpha^{-1}$ and $\tilde{A}$ and $\tilde{B}$ are defined as in (24).

To prove the second claim, $\hat{A}$, $\hat{B}$ and $\hat{c}$ will be constructed such that

$$(31) \qquad \frac{1}{\Delta t^2}(u_{n+1} - 2u_n + u_{n-1}) + \frac{1}{\Delta t}\hat{B}(u_n - u_{n-1}) + \hat{A}u_n = \hat{c}f_n,$$

if and only if (11). Inserting $u_n = Ue^{in\omega\Delta t}$ into (31), results in

$$(32) \qquad \left[\frac{2\cos(\omega\Delta t) - 2}{\Delta t^2} + \frac{i\sin(\Delta t\omega)}{\Delta t}\hat{B} + \frac{1 - \cos(\Delta t\omega)}{\Delta t}\hat{B} + \hat{A}\right] Ue^{in\omega\Delta t} = \hat{c}e^{in\omega\Delta t}F.$$

Using the definitions of α and β and multiplying by α results in the equivalent equation

$$(33) \qquad \left[-\omega^2 + i\omega\frac{\alpha}{\beta}\hat{B} + \frac{\alpha(1 - \cos(\Delta t\omega))}{\Delta t}\hat{B} + \alpha\hat{A}\right] U = \alpha\hat{c}F.$$

This is equivalent to (11) if $\hat{c} = \alpha^{-1}$ and $\hat{A}$ and $\hat{B}$ are defined as in (26). $\qquad\square$

Based on the proposition we define the following time integrators. The time-harmonic solutions with frequency ω of these integrators correspond exactly to time-harmonic solutions of (10).

Definition 2. *Frequency adapted central differences damped leapfrog* will be defined as the time integrator given by

$$(34) \qquad u_{n+1} = I_{\mathrm{acd}}(u_n, u_{n-1}, f_n) := \left(I + \tfrac{1}{2}L\right)^{-1}\left((2 - K)u_n - (I - \tfrac{1}{2}L)u_{n-1} + g_n\right),$$

where K, L and g_n are given by

$$(35) \qquad K = \frac{\Delta t^2}{\alpha}A, \qquad L = \frac{\beta\Delta t}{\alpha}B, \qquad g_n = \frac{\Delta t^2}{\alpha}f_n$$

Frequency adapted backward differences damped leapfrog will be defined as the time integrator given by

$$(36) \qquad u_{n+1} = I_{\mathrm{abd}}(u_n, u_{n-1}, f_n) := (2 - K - L)u_n - (I - L)u_{n-1} + g_n.$$

where K, L and g_n are given by

$$(37) \qquad \begin{aligned} K &= \frac{\Delta t^2}{\alpha}A - \frac{\Delta t\,\beta(1 - \cos(\omega\Delta t))}{\alpha}B \\ L &= \frac{\beta\Delta t}{\alpha}B, \\ g_n &= \frac{\Delta t^2}{\alpha}f_n \end{aligned}$$

The time integrators I_{cd} and I_{acd} are of the same form with different choices for K and L. Therefore for I_{acd} the stability conditions are again (18) and (19), but now with K, L as in (35). Similarly, for I_{abd}, the stability conditions are (18) and (20) with K, L as in (37).

2.2. **Choice of the semi-discrete system and the parameters ω and Δt.** We now look for a second order system of ODE's of the form (10), and a parameter ω such that the time-harmonic solutions to (10) satisfy $HU = F$. Recall that ω is the computational frequency parameter, that is chosen in the construction of the algorithm, and not the physical frequency used in the underlying Helmholtz equation. We will also discuss the choice of time integrator (I_{acd} or I_{abd}) and the choice of the parameter Δt. The requirements are that an explicit and stable scheme is obtained.

Because of (12), we set

$$(38) \qquad A = \operatorname{Re} H + \omega^2 I, \qquad \text{and}$$

$$(39) \qquad B = \omega^{-1} \operatorname{Im} H.$$

where ω is still to be determined.

It is required that the time-integrator leads to explicit scheme for the given matrices A, B. By (39) the matrix B is diagonal if and only if

$$(40) \qquad \operatorname{Im} H \text{ is diagonal.}$$

Following the remarks below (13) the frequency adapted central differences method is used if $\operatorname{Im} H$ is diagonal, and the frequency adapted backward differences method otherwise.

Next the stability conditions must be considered. In case $\operatorname{Im} H$ is diagonal these are given in (18) and (19). Because $\operatorname{Im} H$ is positive semidefinite, L is also positive semidefinite. To ensure that K is positive semidefinite, we set

$$(41) \qquad \omega = \sqrt{-\lambda_{\min}(\operatorname{Re} H)}.$$

(or to a lower bound for $\sqrt{-\lambda_{\min}(\operatorname{Re} H)}$ if this value is not exactly known). The other stability condition (19) is a form of the well-known CFL condition. It implies that the eigenvalues K must be less than 4. For central differences damped leapfrog integration (not frequency adapted) it implies the condition

$$(42) \qquad \Delta t < \frac{2}{\sqrt{\lambda_{\max}(A)}}.$$

For the frequency adapted variant it implies, by (35) and (22) the following condition on Δt

$$(43) \qquad \sin(\frac{\omega \Delta t}{2})^2 < \frac{\omega^2}{\lambda_{\max}(A)},$$

hence

$$(44) \qquad \Delta t < \frac{2}{\omega} \arcsin(\frac{\omega}{\sqrt{\lambda_{\max}(A)}}).$$

The choices and requirements (38), (41) and (44) define a suitable choice of parameters of the systems of ODEs and the I_{acd} integrator in case $\operatorname{Im} H$ is diagonal.

In case that $\operatorname{Im} H$ has nonzero entries outside the diagonal and the I_{abd} integrator is used, the stability conditions are (18) and (20) with K, L as in (37). This results in two conditions that both involve ω and Δt. In this case it is convenient to use $\omega \Delta t$ and Δt as parameters instead of ω and Δt. The parameter $\omega \Delta t$ should be between 0 and π. Given $\omega \Delta t$ the following expression for ω^2 can be derived from the condition that K is positive semidefinite and equation (37)

$$(45) \qquad \omega^2 = -\lambda_{\min}(\operatorname{Re} H) + \frac{\beta}{\omega \Delta t}(1 - \cos(\omega \Delta t))\lambda_{\max}(\operatorname{Im} H)$$

(instead of $\lambda_{\min}(\operatorname{Re} H)$ and $\lambda_{\max}(\operatorname{Im} H)$ lower and upper bounds can be used respectively). From the condition that $4I - K - 2L$ is positive definite we then get the following scalar

condition

$$(46) \qquad \frac{(\omega\Delta t)^2}{\alpha}\left(\frac{\lambda_{\max}(\operatorname{Re} H)}{\omega^2}+1\right)+\frac{\beta}{\alpha}(1+\cos(\omega\Delta t))\frac{\lambda_{\max}(\operatorname{Im} H)}{\omega^2}<4.$$

The following is a stronger inequality than (46)

$$(47) \qquad \left(\frac{\lambda_{\max}(\operatorname{Re} H)}{-\lambda_{\min}(\operatorname{Re} H)}+1\right)(\omega\Delta t)^2+2\frac{\lambda_{\max}(\operatorname{Im} H)}{-\lambda_{\min}(\operatorname{Re} H)}\omega\Delta t<4.$$

From here a value of $\omega\Delta t$ can be obtained that satisfies the conditions by solving a simple quadratic equation. If a larger value of $\omega\Delta t$ is desired, one can look numerically for a value as large as possible for which (46) is still satisfied.

2.3. Time-domain approximate solution operators.
In this section the time-domain approximate solution operator will be defined. We also show that a complex approximate solution can be computed by solving a real time-domain wave equation. This appears to be a standard trick in the field. The main novelty is that the formula for the time-harmonic forcing term (4) is modified so that the forcing is turned on gradually.

The time-domain approximate solution operators will be denoted by S_T^{acd} and S_T^{abd}, depending on which of the integrators I_{acd} and I_{abd} is used. They are defined as follows.

Definition 3. Let $P = \mathrm{acd}$ or $P = \mathrm{abd}$, and assume that I_P is an integrator for the system (10) where A, B and ω satisfy (38). Let χ be a C^∞ function that is non-decreasing, equal to zero for $s \le 0$, and equal to one for $s \ge 1$ and let T be a positive real constant, such that $n_{\mathrm{steps}} := 2\pi\omega^{-1}T/\Delta t$ is an integer. For $F \in \mathbb{C}^N$, let

$$(48) \qquad f_n = f(n\Delta t), \qquad f(t) = \chi(\frac{t}{2\pi\omega^{-1}T})e^{i\omega t}F.$$

The *time-domain approximate solution operator for H* associated with the integrator I_P is the linear map $S_T^P : \mathbb{C}^N \to \mathbb{C}^N$ defined by

$$(49) \qquad S_T^P F = e^{-i2\pi T}u_{n_{\mathrm{steps}}},$$

where u_n, $n = 0, 1, \ldots, n_{\mathrm{steps}}$ is given by

$$(50) \qquad u_{n+1} = I_P(u_n, u_{n-1}, f_n), \qquad u_0 = 0.$$

In section 4 the convergence of $S_T^{\mathrm{acd}}F$ and $S_T^{\mathrm{abd}}F$ to $H^{-1}F$ will be established under the assumption that requirements for stability of the the time integrators discussed in subsection 2.2 are satisfied. Section 5 contains numerical examples for S_T^{acd}.

There is still a lot of freedom to choose the window function χ. In the numerical examples we will introduce therefore an additional parameter ρ, $0 < \rho \le 1$, such that the window function is 1 on $[\rho 2\pi\omega^{-1}T, 2\pi\omega^{-1}T]$ and positive but strictly less than one on $(0, \rho 2\pi\omega^{-1}T)$. We will fix a function χ_1 and set

$$(51) \qquad \chi(s) = \chi_\rho(s) = \chi_1(\rho^{-1}s),$$

The function χ_1 that is used is chosen as a simple sine square window

$$(52) \qquad \chi_1(s) = \begin{cases} 0 & \text{if } s \le 0 \\ \sin(\pi s/2)^2 & \text{if } 0 < s < 1 \\ 1 & \text{if } s \ge 1. \end{cases}$$

The parameter ρ will be called the window parameter.

We next show that it is sufficient to solve a real time-domain wave problem to compute the limiting-amplitude approximate solution. The argument is given in the continuous case, but is applicable equally well in the discrete case.

Let F be a complex right-hand side for the Helmholtz equation and $u(t, x)$ be the solution to (1) with right-hand side $f(t, x) = F(x)e^{i\omega t}$. Assuming the limiting-amplitude principle holds, cf. (5), an approximate solution to the Helmholtz equation is given by

$$(53) \qquad U(x) \approx e^{-i\omega t}u(t, x), \qquad \text{for some large } t.$$

The field $\operatorname{Re} u(t, x)$ can be determined by solving the real wave equation with real forcing term, i.e. with forcing term

$$(54) \qquad \operatorname{Re} F(x)e^{i\omega t} = \cos(\omega t)\operatorname{Re} F(x) - \sin(\omega t)\operatorname{Im} F(x).$$

From (5) it follows that

$$(55) \qquad \operatorname{Re} u(t, x) = \operatorname{Re} U(x)\cos(\omega t) - \operatorname{Im} U(x)\sin(\omega t) + o(1), \qquad t \to \infty.$$

Approximations to $\operatorname{Re} U(x)$ and $\operatorname{Im} U(x)$ can hence be obtained from $\operatorname{Re} u(t, x)$ by

$$(56) \qquad \begin{aligned} \operatorname{Re} U(x) &\approx \operatorname{Re} u(t, x), \qquad t = T\frac{2\pi}{\omega} \\ \operatorname{Im} U(x) &\approx \operatorname{Re} u(t, x), \qquad t = \left(T - \frac{1}{4}\right)\frac{2\pi}{\omega} \end{aligned}$$

with T a large integer. Therefore real time-domain simulation is sufficient.

In the examples Δt is chosen such that the period $2\pi\omega^{-1}$ is an integer multiple of $4\Delta t$. The approximations for $\operatorname{Re} U$ and $\operatorname{Im} U$ in (56) are then easy to compute.

2.4. **Time-domain preconditioned GMRES.**

The approximate Helmholtz solver can be used as a preconditioner for iterative methods like GMRES of BiCGSTAB. Without preconditioning, the system to be solved is $HU = F$. Applying left-preconditioning means that instead the system

$$(57) \qquad PHU = PF$$

is solved, where $P = S_T^{\text{acd}}$ or S_T^{abd}. The right-preconditioned system is

$$(58) \qquad HPV = F.$$

The vector V is solved from this system and the solution to the original problem is then given by $U = PV$. We propose a solution method where GMRES is applied to the left-preconditioned system.

3. Examples

The examples we consider are finite-difference discretizations of the damped Helmholtz equation

$$(59) \qquad -\Delta U - k^2\left(1 - i\frac{\tilde{R}}{\pi}\right)U = F.$$

Here $\tilde{R}$ is the spatially dependent damping in units of damping per cycle. We start with standard second order differences and then apply the method to the discretization from [17].

The method is not limited to finite-difference discretizations. Finite-element discretizations can also lead to linear systems $HU = F$ with H satisfying (8) and (9).

We will see that in our method, the discrete system is a discretization of a modified PDE, see (64) below, and that the CFL bound for this modified PDE is independent of the velocity.

3.1. **Second order finite differences.** It is instructive to start with a simple second order finite-difference discretization. For readability we describe the two-dimensional case. The degrees of freedom will be denoted by $U^{(i,j)}$ (in two dimensions), where i,j are in some rectangular domain $D \subset \mathbb{Z}^2$. The matrix H is defined by the equation

(60)
$$(HU)^{(i,j)} = h^{-2}\left(4U^{(i,j)} - U^{(i-1,j)} - U^{(i+1,j)} - U^{(i,j-1)} - U^{(i,j+1)}\right) - (k^{(i,j)})^2\left(1 - i\frac{\tilde{R}^{(i,j)}}{\pi}\right)U^{(i,j)}$$

where h denotes the grid spacing, and Dirichlet boundary conditions are assumed, i.e. $U^{(i,j)} = 0$ if $(i,j) \notin D$.

In this case $\mathrm{Im}\, H$ is diagonal, and ω and Δt are chosen based on the values

(61)
$$\lambda_{\min}(\mathrm{Re}\, H) = -k_{\max}^2$$
$$\lambda_{\max}(\mathrm{Re}\, H) = -k_{\min}^2 + 8h^{-2}.$$

where

(62)
$$k_{\max} := \max_{(i,j)\in D} k^{(i,j)}, \qquad \text{and} \qquad k_{\min} := \min_{(i,j)\in D} k^{(i,j)}.$$

We find that $\omega = k_{\max}$ while Δt is chosen from (44) using that $\lambda_{\max}(A) = 8h^{-2} + k_{\max}^2 - k_{\min}^2$. The scheme in the computational time domain, can be written as

(63)
$$\frac{\alpha}{\Delta t^2}(u_{n+1}^{(i,j)} - 2u_n^{(i,j)} + u_{n-1}^{(i,j)}) + \frac{\beta}{2\Delta t}\frac{(k^{(i,j)})^2\tilde{R}^{(i,j)}}{\pi k_{\max}}(u_{n+1}^{(i,j)} - u_{n-1}^{(i,j)})$$
$$+ h^{-2}\left(4u_n^{(i,j)} - u_n^{(i-1,j)} - u_n^{(i+1,j)} - u_n^{(i,j-1)} - u_n^{(i,j+1)}\right) + (k_{\max}^2 - (k^{(i,j)})^2)u_n^{(i,j)} = f_n^{(i,j)}.$$

The scheme (63) differs substantially from the standard second order FDTD scheme. In fact, it is a discretization of the PDE

(64)
$$\frac{\partial^2 u}{\partial t^2} - \Delta u + \frac{k^2\tilde{R}}{\pi k_{\max}}\frac{\partial u}{\partial t} + \left(k_{\max}^2 - k^2\right)u = f.$$

This is not necessarily the case. If the operator H would be rescaled, multiplying from the left and the right by a diagonal matrix with entries $c^{(i,j)}$ on the diagonal, then the resulting computational time domain scheme would be close to a standard FDTD scheme.

This leads to a different behavior of the CFL bound and the minimum number of timesteps per period. In standard schemes the CFL bound is chosen based on the maximum velocity, but the grid spacing based on the minimum velocity, this results in a rough equality.

(65) $$(\text{\# timesteps per period}) \lesssim \frac{c_{\max}}{c_{\min}}(\text{min \# gridpoints per wavelength})$$

For the new scheme (63) we have

(66) $$(\text{\# timesteps per period}) \lesssim (\text{min \# gridpoints per wavelength}).$$

For standard schemes, the CFL bound is locally suboptimal, where the velocity is below the maximum. For the modified PDE (64) on the other hand, the CFL bound is locally optimal or near-optimal throughout the domain.

3.2. **An optimized finite-difference method.** Next we consider a discretization with a 27 point cubic stencil (in 3-D) that was described in [17]. There exists different variants of such compact stencil methods, see among others [2, 20, 23]. For each gridpoint, the number of neighbors that the gridpoint interacts with is relatively small (when compared e.g. to higher order finite elements). Even so, the dispersion errors of these schemes are

also relatively small, as shown in [17], so that these methods can be used with relatively coarse meshes[1].

The equation discretized in [17] was the real part of (59). We will discuss here the situation with constant k, for variable k we refer to appendix B. The stencil is the 27 point cube that we will denote with $\{-1, 0, 1\}^3$. For constant k, due to symmetry there are four different matrix coefficients. The values of these coefficients are $h^{-2} f_s(\frac{hk}{2\pi})$, for $s = 0, 1, 2, 3$ respectively, where the dimensionless function f_s describes the coefficient as a function of the dimensionless quantity $\frac{hk}{2\pi}$. To be precise,

$$(67) \quad (\mathrm{Re}\, H)^{(i,j,l;p,q,r)} = \begin{cases} \frac{1}{h^2} f_{|i-p|+|j-q|+|l-r|}(\frac{hk}{2\pi}) & \text{if } (i-p, j-q, l-r) \in \{-1, 0, 1\}^3 \\ 0 & \text{otherwise} \end{cases}$$

In [17] the f_s are precomputed functions, in a class of piecewise polynomial functions, obtained by optimization to minimize phase errors. For the 2-D case, in [2] explicit expressions for the optimal functions f_s, $s = 0, 1, 2$ were derived. The imaginary part was discretized as above, i.e. it was diagonal with entries $\frac{(k^{(i,j,l)})^2 \tilde{R}^{(i,j,l)}}{\pi}$.

Because $\mathrm{Im}\, H$ is diagonal, the integrator I_{acd} is used. The discretization in [17] has in addition the property that it was second order and such that

$$(68) \qquad\qquad \mathrm{Re}\, H + k^2 I \text{ is symmetric positive definite.}$$

Thus in case of constant k

$$(69) \qquad\qquad \omega = k.$$

The upperbound for $\mathrm{Re}\, H$ that determines the maximum for Δt is given by

$$(70) \qquad \lambda_{\max}(\mathrm{Re}\, H) = f_0(\frac{kh}{2\pi}) - 6 f_1(\frac{kh}{2\pi}) + 12 f_2(\frac{kh}{2\pi}) - 8 f_3(\frac{kh}{2\pi}).$$

This bound is typically somewhat less than the bound associated with second order finite differences with the same parameters. It is straightforward to follow the recipe of subsection 2.2. For this scheme we have again (66), and it can be considered a discretization of (64) rather than of (1).

4. Analysis

Here theoretical results will be obtained concerning the stability of the time integrators defined in subsection 2.1, the solutions of these time-integration schemes and and the convergence of the approximate solution operators defined in subsection 2.3.

The consequences of the stability analysis for the choice of Δt were already discussed in subsection 2.2.

4.1. **Stability.** To study the conditions under which (16) and (34) are stable, we study the growth of the solutions to the homogeneous recursion

$$(71) \qquad (1 + \tfrac{1}{2}L)u_{n+1} + (-2 + K)u_n + (I - \tfrac{1}{2}L)u_{n-1} = 0.$$

Throughout we will assume that K and L are symmetric matrices and that L is positive semidefinite. The basic idea is to show that the following energy functions stays bounded

$$(72) \quad E_{\mathrm{cd}}(n - 1/2) = \langle u_n - u_{n-1}, (4I - K)(u_n - u_{n-1}) \rangle + \langle u_n + u_{n-1}, K(u_n + u_{n-1}) \rangle.$$

Here $\langle \cdot, \cdot \rangle$ denotes the standard inner product. If the energy function is coercive, than the solution also stays bounded. The following theorem, states the stability conditions that follow from such an analysis. The conditions under (ii) in the theorem were already mentioned above, see equations (18), (19).

---

[1] In some applications relatively coarse meshes are used to save on computation time. Reduction of dispersion errors is important in this case. In general, other discretization errors can also be present, e.g. related to the presence of variable coefficients.

Theorem 1. *Let u_n, $n \in \mathbb{Z}$ be a solution to the homogeneous recursion (71), where K and L are real valued symmetric matrices and L is positive semidefinite.*

(i) *If K and $4I - K$ are positive definite then E_{cd} is equivalent to a norm on $\mathbb{R}^{2N}$. If $L = 0$ then E_{cd} is conserved and solutions remain bounded if $t \to \pm\infty$. If L is positive semidefinite then $\Delta E_{\mathrm{cd}}(n) \leq 0$ and solutions remain bounded if $t \to \infty$.*

(ii) *If K is positive semidefinite and $4I - K$ is positive definite and K has one or more zero eigenvalues then E_{cd} is not equivalent to a norm. If $L = 0$ then E_{cd} is conserved and solutions grow at most linearly if $t \to \pm\infty$. If L is positive semidefinite, then $\Delta E_{\mathrm{cd}}(n) \leq 0$ and solutions grow at most linearly if $t \to \infty$.*

Proof. To prove the result, a bound is derived for

$$\Delta E_{\mathrm{cd}}(n) = E_{\mathrm{cd}}(n + 1/2) - E_{\mathrm{cd}}(n - 1/2). \tag{73}$$

Using that K is symmetric in combination with basis rules for standard products results in

$$\begin{aligned} \Delta E_{\mathrm{cd}}(n) = &\langle u_{n+1} - 2u_n + u_{n-1}, (4I - K)(u_{n+1} - u_{n-1})\rangle \\ &+ \langle u_{n+1} - u_{n-1}, K(u_{n+1} + 2u_n + u_{n-1})\rangle. \end{aligned} \tag{74}$$

By using the recursion equation in two places results one obtains the estimate

$$\begin{aligned} \Delta E_{\mathrm{cd}}(n) = &\langle -Ku_n - \tfrac{1}{2}L(u_{n+1} - u_{n-1}), (4I - K)(u_{n+1} - u_{n-1})\rangle \\ &+ \langle u_{n+1} - u_{n-1}, 4Ku_n + K(-Ku_n - \tfrac{1}{2}L(u_{n+1} - u_{n-1}))\rangle \\ = &-2\langle u_{n+1} - u_{n-1}, L(u_{n+1} - u_{n-1})\rangle \\ \leq &\, 0, \end{aligned} \tag{75}$$

where the last inequality holds because by assumption L is positive semidefinite. The theorem follows from this result. $\qquad\square$

To establish stability of backward differences damped leapfrog, we study the growth of solutions to the recursion

$$u_{n+1} + (-2 + K + L)u_n + (I - L)u_{n-1} = 0 \tag{76}$$

using the energy function

$$\begin{aligned} E_{\mathrm{bd}}(n - 1/2) = &\langle u_n - u_{n-1}, (4I - K)(u_n - u_{n-1})\rangle + \langle u_n + u_{n-1}, K(u_n + u_{n-1})\rangle \\ &- 2\langle u_n - u_{n-1}, L(u_n - u_{n-1})\rangle. \end{aligned} \tag{77}$$

Theorem 2. *Let u_n, $n \in \mathbb{Z}$ be a solution to the homogeneous recursion (76), where K and L are real valued symmetric matrices.*

(i) *If K and $4I - K - 2L$ are positive definite, then E_{bd} is equivalent to a norm on $\mathbb{R}^{2N}$. If $L = 0$ then E_{bd} is conserved and solutions remain bounded if $t \to \pm\infty$. If L is positive semidefinite then $\Delta E_{\mathrm{bd}}(n) \leq 0$ and solutions remain bounded if $t \to \infty$.*

(ii) *If instead K is positive semidefinite with one or more zero eigenvalues and $4I - K - 2L$ is positive definite, then E_{bd} is not equivalent to a norm. If $L = 0$ then E_{bd} is conserved and solutions grow at most linearly if $t \to \pm\infty$, If L is positive semidefinite, then $\Delta E_{\mathrm{bd}}(n) \leq 0$ and solutions grow at most linearly if $t \to \infty$.*

Proof. Similarly as in (72) define

$$\Delta E_{\mathrm{bd}}(n) = E_{\mathrm{bd}}(n + 1/2) - E_{\mathrm{bd}}(n - 1/2). \tag{78}$$

Using that K is symmetric in combination with basis rules for standard products results in

$$\begin{aligned} \Delta E_{\mathrm{bd}}(n) = &\langle u_{n+1} - 2u_n + u_{n-1}, (4I - K)(u_{n+1} - u_{n-1})\rangle \\ &+ \langle u_{n+1} - u_{n-1}, K(u_{n+1} + 2u_n + u_{n-1})\rangle \\ &- 2\langle u_{n+1} - u_n, L(u_{n+1} - u_n)\rangle + 2\langle u_n - u_{n-1}, L(u_n - u_{n-1})\rangle. \end{aligned} \tag{79}$$

By using the recursion equation in two places results one obtains the estimate

$$
\begin{aligned}
\Delta E_{\mathrm{bd}}(n) = {} & \langle -Ku_n - L(u_n - u_{n-1}), (4I - K)(u_{n+1} - u_{n-1}) \rangle \\
& + \langle u_{n+1} - u_{n-1}, 4Ku_n + K(-Ku_n - L(u_n - u_{n-1})) \rangle \\
& - 2\langle u_{n+1} - u_n, L(u_{n+1} - u_n) \rangle + 2\langle u_n - u_{n-1}, L(u_n - u_{n-1}) \rangle \\
= {} & -4\langle u_{n+1} - u_{n-1}, L(u_n - u_{n-1}) \rangle \\
& - 2\langle u_{n+1} - u_n, L(u_{n+1} - u_n) \rangle + 2\langle u_n - u_{n-1}, L(u_n - u_{n-1}) \rangle \\
= {} & -2\langle u_{n+1} - u_{n-1}, L(u_{n+1} - u_{n-1}) \rangle \\
\leq {} & 0,
\end{aligned}
$$
(80)

where the last inequality holds because by assumption L is positive semidefinite. The theorem follows from this result. $\qquad\square$

4.2. **Eigenvalue analysis.** An analysis based on the eigenvalues of K gives insight in the question whether these conditions are necessary. Suppose v is an eigenvector of K with eigenvalue k and simultaneously an eigenvector of L with eigenvalue ℓ. One can think of the situation that $L = \ell I$. We start by looking for solutions to equation (71) of the form $u_n = \Lambda^n v$. The constant Λ must then satisfy

$$
(1 + \ell/2)\Lambda^2 + (-2 + k)\Lambda + (1 - \ell/2) = 0. \tag{81}
$$

The solution to this equation are

$$
\Lambda_{\pm} = \frac{-1 + k/2}{1 + \ell/2} \pm \frac{1}{1 + \ell/2}\sqrt{-k + k^2/4 + \ell^2/4} \tag{82}
$$

We consider the growth of solutions, first if $\ell = 0$ (no damping). Then if $0 < k < 4$ both solutions are complex with $|\Lambda_{\pm}| = 1$. If $k = 0$ then (71) has solutions $u_n = C_1 v + C_2 n v$. If $k < 0$ or $k > 4$ at least one of $\Lambda_{\pm}$ has modulus larger than 1. Next consider the case $\ell > 0$ (damping present). If $0 < k < 4$ then $\Lambda_{\pm}$ can be complex (small damping) or real (large damping), with $|\Lambda_{\pm}| < 1$ in both cases. If $k = 0$ or $k = 4$ one $\Lambda_{\pm}$ is equal to 1 and the other smaller than 1. If $k < 0$ or $k > 4$, exponentially growing solutions exist. For stability, K and $4I - K$ need to be positive semidefinite, but we will require $4I - K$ to be strictly positive definite (to avoid the solution with $\Lambda = -1$ while $k = 4$, $\ell > 0$).

Next we study the undamped solutions in case the eigenvectors of L are not those of K. In this case, the recursion (71) can be written in first order form. Let

$$
y_n = \begin{bmatrix} u_{n-1} \\ u_n \end{bmatrix}, \qquad g_n = \begin{bmatrix} 0 \\ f_n \end{bmatrix}, \tag{83}
$$

and

$$
\Xi = \begin{bmatrix} 0 & I \\ -(I + L)^{-1}(I - L) & (I + L)^{-1}(2I - K) \end{bmatrix} \tag{84}
$$

then the integrators I_{cd} and I_{acd} from definitions 1 and 2 can be written as

$$
y_{n+1} = \Xi y_n + g_n. \tag{85}
$$

The properties of the solutions are directly related to the eigenvalues, (generalized) eigenvectors and the Jordan blocks of Ξ. We next list some properties of Ξ that relate to eigenvalues ξ of Ξ with $|\xi| = 1$. These correspond to undamped solutions. The basic idea is to show that there are not more of these than there should be.

Theorem 3. *Assume (18), (19). The following properties hold for the eigenvalues, (generalized) eigenvectors and Jordan blocks of Ξ:*

(i) all eigenvectors are of the form $[u, \xi u]$, with $u \in \mathbb{C}^N$;
(ii) there are no eigenvalues $\xi = -1$;
(iii) for $|\xi| = 1$, $\xi \neq 1$ there are no Jordan blocks of size > 1;

(iv) for $|\xi| = 1$, $\xi \neq 1$ the u in $[u, \xi u]$ is in $\ker L$, and is an eigenvector of K and ξ follows from (82);

(v) for $\xi = 1$, there are no Jordan blocks of size > 2, an eigenvector is of the form $v = [u, u]$ with $u \in \ker K$ and if w is a generalized eigenvector such that $\Xi w = w + v$, v an eigenvector, then $v = [u, u]$ with u also in $\ker L$, and $w = [w_1, w_1 + u]$ with $w_1 \in \ker K$.

Proof. Claim (i) is obvious.

Regarding (ii), the equations $\Xi[u, \xi u]^T = \xi[u, \xi u]^T$ with $\xi = -1$ gives $(4I - K)u = 0$ which is impossible because $4I - K$ is positive definite by assumption.

Claim (iii) follows from the energy growth equations. Solution to second order recursion would be of the form $u_n = \xi^n w + n\xi^{n-1}v$, and the dominant term in the energy in the limit $n \to \infty$ would be $\langle n(1 - \xi)v, (4I - K)n(1 - \xi)v \rangle$. This term would be unbounded as $n \to \infty$ which is impossible, hence any Jordan block of size > 1 must be associated with an eigenvalue $\xi = 1$.

In the situation of claim (iv), solutions are of the form $u_n = \xi^n v$ with $v \in \mathbb{C}^N$. Energy must be conserved hence $\langle u_{n+1} - u_{n-1}, L(u_{n+1} - u_{n-1}) \rangle = 0$ hence hence $(\xi - \xi^{-1})u \in \ker L$, hence $u \in \ker L$. But then it follows that $Ku = (-\xi^{-1} + 2 - \xi)u$, so that u is a simultaneous eigenvector of K, and L.

The first part of part (v) follows from the bound on the energy. Jordan blocks of size > 2 would lead to solutions of the form

$$(86) \qquad\qquad u_n = w^{(2)} + nw^{(1)} + n(n-1)v,$$

The dominant contribution to the term $\langle u_n - u_{n-1}, (4I - K)(u_n - u_{n-1}) \rangle$ would be $\langle 2(n-1)v, (4I - K)2(n-1)v \rangle$, which would be unbounded, which is not possible. The second part of (v) follows from the form of Ξ. If eigenvector is $V = [v_1, v_2]^T$, $v_j \in \mathbb{C}^N$, then $v_1 = v_2$ and

$$(87) \qquad\qquad -(1 - L)v_1 + (2I - K)v_1 = (1 + L)v_1$$

hence $Kv_1 = 0$. The third part of (v) follows from the form of Ξ. Working out the first line of equation $\Xi w = w + v$ yields $w_2 = w_1 + u$, working out the second line gives $Lu = 0$. $\qquad\square$

4.3. Convergence of the approximate solution operators S_T^{acd} and S_T^{abd}.

In this subsection we will write $u(n\Delta t)$ instead of u_n and $f(n\Delta t)$ instead of f_n. Instead of the two-sided sequences (u_n) and (f_n) we write $u(t)$, $f(t)$, with $t \in \Delta t\mathbb{Z}$. The Fourier transform from functions on $\Delta t\mathbb{Z}$ to functions on $\mathbb{T}_{2\pi/\Delta t}$ is as defined in appendix A.

Associated with the integrator I_{acd} is a second order difference operator C_{acd}. We define this operator as follows

$$(88) \qquad C_{\mathrm{acd}}(u)(t) = \frac{\alpha}{\Delta t^2}\left[(1 + \tfrac{1}{2}L)u(t + \Delta t) + (-2 + K)u(t) + (I - \tfrac{1}{2}L)u(t - \Delta t)\right]$$

where K, L are as defined in (35). Solutions to the time-integration satisfy

$$(89) \qquad\qquad C_{\mathrm{acd}}(u)(t) = f(t).$$

The left-hand side can be see as the convolution of u with a kernel Γ_{acd} that is a matrix valued function on $\Delta t\mathbb{Z}$. (The explicit expression for Γ_{acd} is easily derived from (88).) In the Fourier domain the convolution becomes a multiplication and we have

$$(90) \qquad\qquad \widehat{\Gamma}_{\mathrm{acd}}(\tau)\widehat{u}(\tau) = \widehat{f}(\tau).$$

From proposition 1 it follows that

$$(91) \qquad\qquad \widehat{\Gamma}_{\mathrm{acd}}(\omega) = -\omega^2 I + i\omega B + A.$$

In addition we know that $\widehat{\Gamma}$ is C^∞, because Γ is nonzero only for $t \in \{-\Delta t, 0, \Delta t\}$.

By $\Phi_{\mathrm{acd}}(t)$, $t \in \Delta t\mathbb{Z}$ we will denote the causal Green's function associated with (89). It is a function $\Delta t\mathbb{Z} \to \mathbb{C}^{N \times N}$ defined as the solution to

$$(92) \qquad C_{\mathrm{acd}}\Phi_{\mathrm{acd}}(t) = I\delta(t), \qquad \text{and} \qquad \Phi_{\mathrm{acd}}(t) = 0 \text{ if } t \leq 0,$$

where $\delta(t)$ is as defined in appendix A. Assuming that the conditions in (18), (19) hold, Φ_{acd} grows at most polynomially if $t \to \infty$ (by Theorem 1), and its Fourier transform $\widehat{\Phi}_{\mathrm{acd}}$ is well defined as a matrix valued distribution on the circle $\mathbb{T}_{2\pi/\Delta t}$.

We will first show that the approximate solution operator S_T^{acd} can be expressed as a weighted mean of $\widehat{\Phi}(\tau)$ around $\tau = \omega$. For this purpose we define a helper function ϕ_ϵ, depending on χ, as follows

$$(93) \qquad \psi_T(t) = \chi(1 - \left| \frac{t}{2\pi\omega^{-1}T} \right|), \qquad \text{and} \qquad \phi_\epsilon(\tau) = \frac{1}{2\pi}\mathcal{F}\psi_{1/\epsilon}(\tau).$$

Note that ϕ_ϵ is an approximation to the identity. We have the following result

Theorem 4. *Assume ϕ_ϵ and Φ_{acd} are as just defined, then*

$$(94) \qquad S_T^{\mathrm{acd}} = \phi_{1/T} * \widehat{\Phi}_{\mathrm{acd}}(\omega).$$

In words, s_T^{acd} equals the convolution product of $\phi_{1/T}$ and $\widehat{\Phi}_{\mathrm{acd}}$, evaluated at $\tau = \omega$. The convolution product is taken on the torus $\mathbb{T}_{2\pi/\Delta t}$.

Proof. Let $\tilde{T} = 2\pi\omega^{-1}T$. By linearity, the time-domain approximate solution $S_T(F)$ satisfies

$$(95) \qquad S_T^{\mathrm{acd}}(F) = e^{-i\omega\tilde{T}}\Delta t \sum_{t \in \Delta t\mathbb{Z}, 0 \leq t < \tilde{T}} \Phi(\tilde{T} - t)\chi(t/\tilde{T})e^{i\omega t}F$$

Inserting the definition of ψ_T this becomes

$$(96) \qquad S_T^{\mathrm{acd}}(F) = \left[\Delta t \sum_{t \in \Delta t\mathbb{Z}} \Phi(\tilde{T} - t)\psi_T(\tilde{T} - t)\chi(t/\tilde{T})e^{-i\omega(\tilde{T}-t)} \right] F = \left[\mathcal{F}(\psi_T\Phi)(\omega)\right] F.$$

The equality (94) follows because the Fourier transform of the product is $\frac{1}{2\pi}$ times the convolution product of the Fourier transforms, see (115). $\square$

Concerning the convergence of the time-domain approximate solutions to the correct solutions we have the following result.

Theorem 5. *If*

$$(97) \qquad H = -\omega^2 I + i\omega B + A \text{ is non-singular}$$

and A, B, ω and Δt are such that K, L defined in (35) satisfy the stability conditions (18) and (19) then

$$(98) \qquad \lim_{T \to \infty} S_T^{\mathrm{acd}} = H^{-1}.$$

Proof. The Fourier transform $\widehat{\Phi}_{\mathrm{acd}}$ satisfies

$$(99) \qquad \widehat{\Gamma}_{\mathrm{acd}}(\tau)\widehat{\Phi}_{\mathrm{acd}}(\tau) = I.$$

Note that $\widehat{\Gamma}_{\mathrm{acd}}(\tau)$ is a C^∞ function and $\widehat{\Phi}_{\mathrm{acd}}$ is a distribution and that this equality is in the sense of distributions.

By the assumption (97) and the property (91), the matrix valued function $\widehat{\Gamma}_{\mathrm{acd}}(\tau)$ is non-singular on a neighborhood of $\tau = \omega$. It follows that $\widehat{\Phi}_{\mathrm{acd}}(\tau)$ is continuous on a neighborhood of $\tau = \omega$ and that

$$(100) \qquad \widehat{\Phi}_{\mathrm{acd}}(\omega) = \widehat{\Gamma}_{\mathrm{acd}}(\omega)^{-1} = H^{-1}.$$

Because ϕ_ϵ is an approximation to the identity and $\widehat{\Phi}(\tau)$ is continuous at $\tau = \omega$, it follows from theorem 4 and standard results in integration theory and distribution theory that

$$(101) \qquad\qquad \lim_{T\to\infty} S_T^{\mathrm{acd}} = \widehat{\Phi}(\omega) = H^{-1}. \qquad\qquad \square$$

A similar analysis can be performed for the approximate solution operator S_T^{abd}. The equivalent of (88) is

$$(102) \qquad C_{\mathrm{abd}}(u)(t) = \frac{\alpha}{\Delta t^2}\left[u(t+\Delta t) + (-2+K+L)u(t) + (I-L)u(t-\Delta t)\right]$$

where K, L are as defined in (37). A causal Green's function Φ_{abd} is defined satisfying

$$(103) \qquad C_{\mathrm{abd}}\Phi_{\mathrm{abd}}(t) = I\delta(t), \qquad \text{and} \qquad \Phi_{\mathrm{abd}}(t) = 0 \text{ if } t \le 0,$$

The following theorems are proved in the same ways as theorems 4 and 5

Theorem 6. *Assume ϕ_ϵ and Φ_{abd} are as just defined, then*

$$(104) \qquad\qquad S_T^{\mathrm{abd}} = \phi_{1/T} * \widehat{\Phi}_{\mathrm{abd}}(\omega).$$

Theorem 7. *If*

$$(105) \qquad\qquad H = -\omega^2 I + i\omega B + A \text{ is non-singular}$$

and A, B, ω and Δt are such that K, L defined in (37) satisfy the stability conditions (18) and (20) then

$$(106) \qquad\qquad \lim_{T\to\infty} S_T^{\mathrm{abd}} = H^{-1}.$$

5. Numerical examples

In this section we study some examples. The examples all involve an optimized finite-difference discretization described in subsection 3.2 in two and three dimensions.

To study the 2-D method, a simple implementation in Julia was made. For the 3-D case a mixed Julia/C implementation was made. In this case the time stepping was done in C, the computation of coefficients and the GMRES iteration were done in Julia. In the C implementation, for each grid point and timestep, 14 real coefficients had to be read, of which one also had to be written back to. The C implementation used AVX extensions but was otherwise straightforward. In most computations double precision numbers were used. The exception was the time-stepping performed in C. We found that the time-domain preconditioner could also be run in single precision, since the GMRES solver would automatically take care of rounding errors in subsequent iterations.

5.1. **2-D examples.** We considered three 2-D examples: A constant velocity model and two piecewise constant models defined on the unit square. The first of the two piecewise constant models allows for resonances in the circular region. On the exterior of the model damping layers of thickness 32 gridpoints were added to simulate an unbounded domain. The simulations in these examples were done using a minimum of 6 points per wavelength. In each case this resulted in 8 timesteps per period. See figure 1 for non-constant velocity models and some solutions in these models.

The first objective was to the study the convergence of the approximate solution $S_T^{\mathrm{acd}}F$ to $H^{-1}F$. For this we took models of size 320×320 and 640×640 (excluding damping layers), and let the right-hand side be a point source. The "taper" parameter ρ was varied, we considered values in $\{0, 0.25, 0.5, 0.75\}$. The value 0 was not exactly zero, in this case the time-harmonic right-hand side grew from 0 to 1 over one period. The convergence (relative difference between approximate and true solutions) is given in Figure 2. Note the differing axes in the Figure 2(b). The main conclusions from these figures are that the convergence in the resonant model is relatively poor, and that the choice of $\rho = 0$ (no
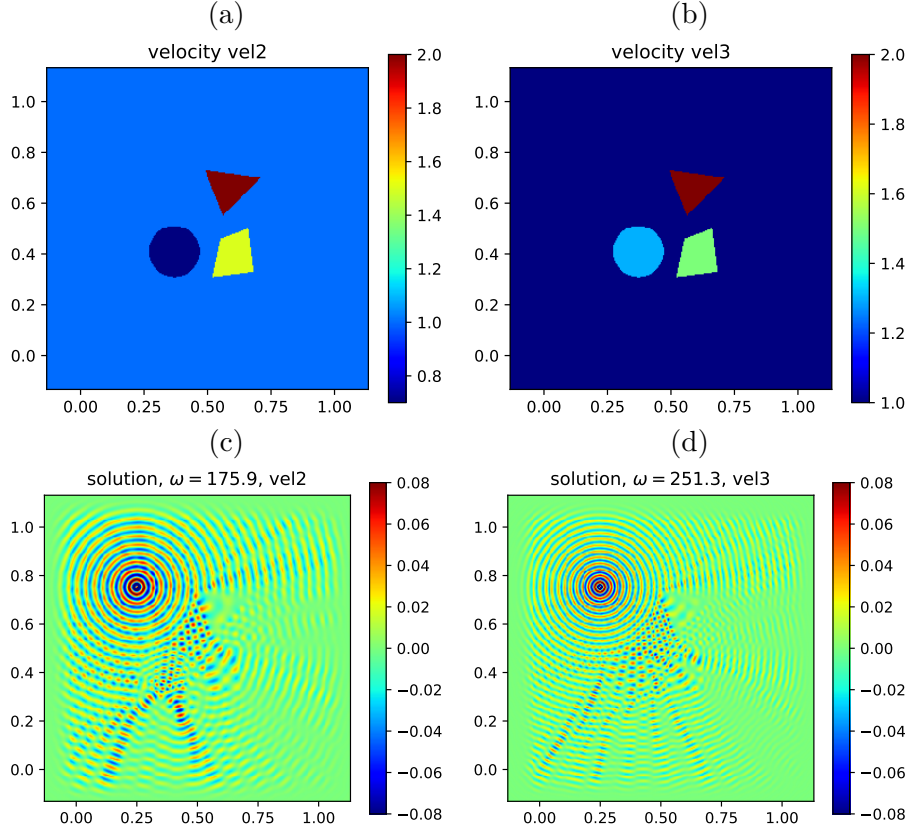
FIGURE 1. Two velocity models (a,b) and solutions in these models (c,d). A relatively small example of 240×240 was used so that the wavefield oscillations are still visible.

tapering) leads to poor convergence. The detailed amount of tapering is less important. The lower value ($\rho = 0.25$) appears to perform best unless extremely small relative errors are required.

GMRES convergence for the three velocity models of size 640 gridpoints (excluding damping layers) are given in Figure 3. In each case the number of periods of the preconditioner was varied. In Figures 3(a-c) the taper parameter was 0.25 and both the error indicator from GMRES and the true error are plotted. In Figure 3(d) the GMRES error was plotted and the taper parameter was varied. On the x axis, the number of iterations time the number of periods per iteration was displayed. This is roughly, but not quite proportional to the cost, the main difference being that one more preconditioner application is needed for the right-hand side in the preconditioned system. In velocity models 1 and 3, there was no speedup compared to the direct application of the time-domain solver. Neither was the method much slower. However, in the resonant velocity model (velocity model 2), the performance using GMRES was substantially better than when the time-domain solver was used directly.

In the examples about 50 to 100 periods for the preconditioner worked best. This is approximately the size of the example in wavelenghts.

5.2. **Examples in 3-D.** We also studied the performance of the algorithm in three dimensions. In this case, the velocity model was the SEG/EAGE Salt Model. This is a standard, non-resonant synthetic model in the geophysics community. In this case our goal was to obtain a first estimate of the computational cost of the method. A minimum of 6 gridpoints per wavelength was used. The Julia/C code was run on a 2019 MacBook
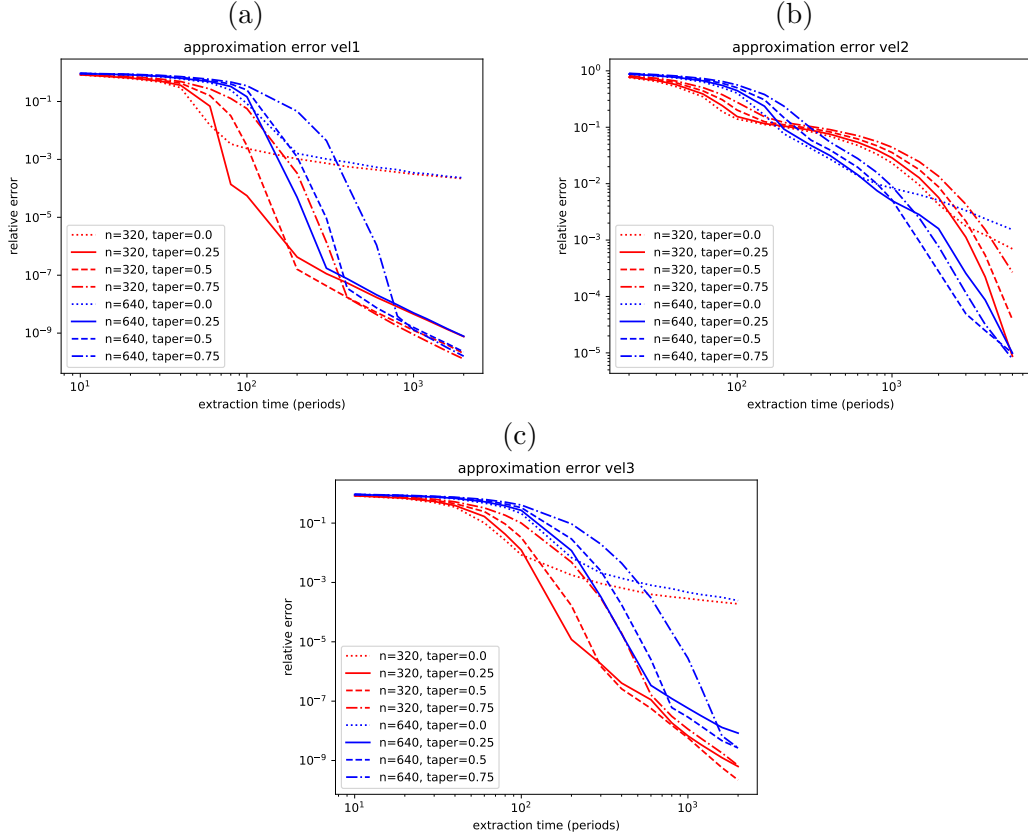
(a)   (b)

(c)

FIGURE 2. Convergence behavior of large time approximate solutions. Note the different scales in figure (b).

physical frequency	2.5 Hz	4 Hz	6 Hz
problem size	$200 \times 200 \times 106$	$280 \times 280 \times 130$	$392 \times 392 \times 165$
degrees of freedom	4.24 e6	1.02 e7	2.54 e7
time steps/period	8	8	8
periods/iteration	25	40	60
taper parameter	0.25	0.25	0.25
iterations	6	6	6
computation time	45 s	166 s	601 s

TABLE 1. Computational results for the SEG/EAGE Salt model

Pro with a 2.6 GHz 6-core Intel i7 processor and 16 GB main memory. A GMRES error reduction with a factor 10^{-5} was required. The results are in Table 5.2.

6. GENERALIZATIONS

As outlined in the introduction, the new time-domain preconditioned GMRES solver is based on four innovative ideas: A modified semi-discrete system derived from the discrete Helmholtz equation (equation (10)), a new time-integration scheme, introduction of a smooth window in the computation of limiting-amplitude solutions and the use of the time-domain approximate solution operator as a preconditioner.

Some of these ideas can be used separately. The new semi-discrete system and the new integration method could be used with the exact controllability or WaveHoltz methods.
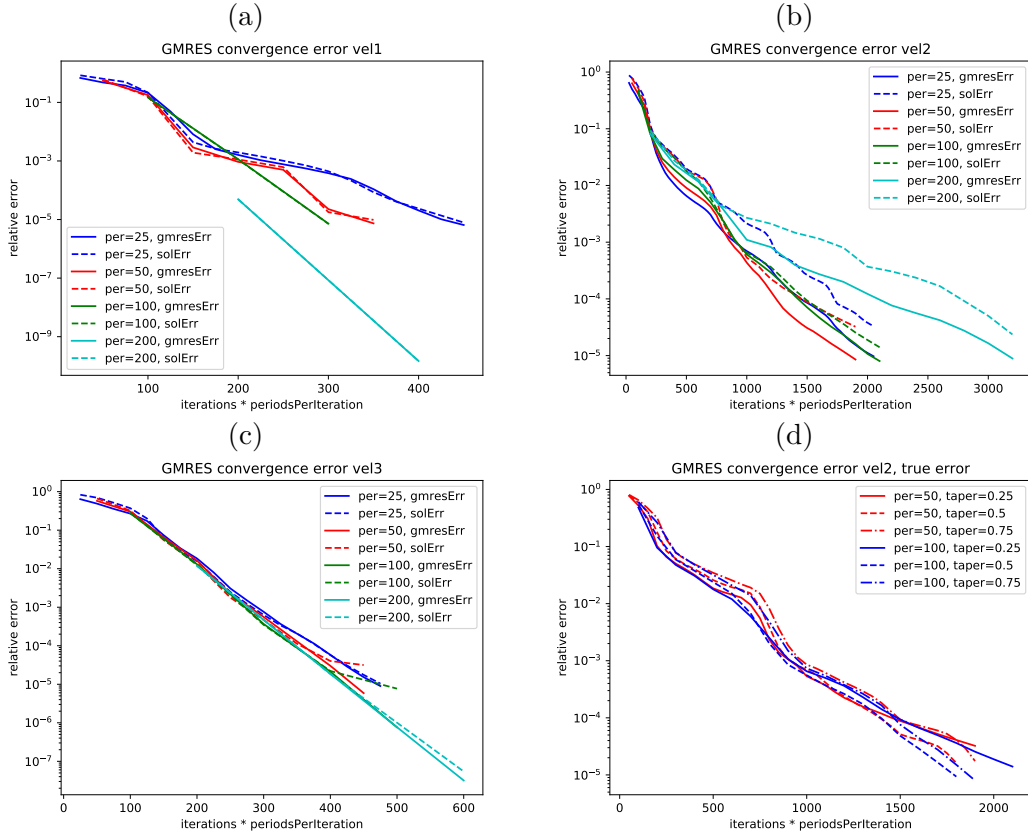
FIGURE 3. Preconditioned GMRES convergence for different models and different parameter choices

In this section we discuss the application of Krylov subspace method in combination with a different semi-discrete equation and time integrator.

We assume the semi-discrete system is still of the form (10). Denoting

$$(107) \qquad v = \begin{bmatrix} u \\ \frac{\partial u}{\partial t} \end{bmatrix}, \qquad g = \begin{bmatrix} 0 \\ f \end{bmatrix}, \qquad \Xi = \begin{bmatrix} 0 & I \\ -A & -B \end{bmatrix}$$

this can be written in first order form

$$(108) \qquad \frac{\partial v}{\partial t} = \Xi v + g.$$

The first order system can be discretized for example using a standard fourth order Runge-Kutta method, which yields

$$(109) \quad \begin{aligned} v_{n+1} &= (I + h\Xi + \frac{h^2}{2}\Xi^2 + \frac{h^3}{6}\Xi^3 + \frac{h^4}{24}\Xi^4)v_n \\ &+ \frac{h}{24}(4 + 4h\Xi + 2h^2\Xi^2 + h^3\Xi^3)g_n + \frac{h}{12}(8 + 4h\Xi + h^2\Xi^2)g_{n+1/2} + \frac{h}{6}g_{n+1} \end{aligned}$$

Requiring that $v_n = e^{in\omega\Delta t}V$ and $g_n = e^{in\omega\Delta t}G$ leads to the following equation for V and G

$$(110) \quad \begin{aligned} &\left[e^{i\omega\Delta t}I - I - h\Xi - \frac{h^2}{2}\Xi^2 - \frac{h^3}{6}\Xi^3 - \frac{h^4}{24}\Xi^4 \right]V = \\ &\left[\frac{h}{24}(4I + 4h\Xi + 2h^2\Xi^2 + h^3\Xi^3) + e^{i\omega\Delta/2}\frac{h}{12}(8I + 4h\Xi + h^2\Xi^2) + e^{i\omega\Delta t}\frac{h}{6}I \right]G. \end{aligned}$$

This is the exact discrete Helmholtz equation satisfied by the periodic solutions of the discrete-time-and-space system. Based on the experience in this paper, this system could be solved by GMRES preconditioned by a time-domain preconditioner defined as in subsection 2.3 but applied to (108) solved by RK4. For different Runge-Kutta integrators, different polynomials in front of V and G result, but the principle is the same.

7. Concluding remarks

In this paper we constructed a time-domain preconditioner for certain indefinite linear systems, and studied its properties and behavior analytically and with numerical examples. It should be emphasized that the method does not compute in the physical time domain. We call it a time-domain method, because of the similarity with classical time-domain methods for time-harmonic waves.

For the practical application it would be useful to have further examples and a comparison with alternatives, and more insight into how the method behaves for different choices of H, e.g. for different discretizations. We will make a few brief remarks in this direction.

First it is clear that the method requires relatively little memory, compared to alternatives that use LU (or LDL^T) decompositions, such as domain-decomposition and direct methods, see [18, 14] and references in [8]. In the 3-D implementation here, with GMRES with restart $n_r = 10$, most memory was used for the approximately $n_r + 2$ complex double precision vectors needed for GMRES. This was in part because the timestepping was done in single precision, and using real fields. Memory use could be somewhat reduced by setting $n_r = 5$ or using a different iterative method like BiCGSTAB.

For finite element discretizations the cost in general will be different. These methods often have stricter CFL bounds, and there may be more nonzero matrix elements, depending on the order of the finite elements, which leads to larger cost. In case of unstructured meshes computations in general are less efficient, because there is more indirect memory access and cache misses. On the other hand, the size of the grid cells can be adapted to the local velocity which means the number of grid cells can be smaller.

It is difficult to compare performance of different methods, as methods are run on different computer systems, with different examples and implementations are optimized to different degrees. We refer to [1, 7, 13, 14, 18, 22, 24] for some alternative methods. We believe that computation times of the method as outlined are modest, and there is potential for further improvements, by using GPUs or by reorganizing the code to better make use of cached data. It remains challenging to get the most out of modern computer hardware in time-domain finite-difference and finite-element simulations. We hope that recent developments in this area, cf. [12], will lead to further improvements.

References

[1] D. Appelo, F. Garcia, and O. Runborg. Waveholtz: Iterative solution of the Helmholtz equation via the wave equation, 2019.

[2] I. Babuška, F. Ihlenburg, E. T. Paik, and S. A. Sauter. A generalized finite element method for solving the Helmholtz equation in two dimensions with minimal pollution. *Comput. Methods Appl. Mech. Engrg.*, 128(3-4):325–359, 1995.

[3] J. Berland, C. Bogey, and C. Bailly. Low-dissipation and low-dispersion fourth-order Runge–Kutta algorithm. *Computers & Fluids*, 35(10):1459–1463, 2006.

[4] B.R. Vainberg. Limiting-amplitude principle. Encyclopedia of Mathematics. URL: `http://www.encyclopediaofmath.org/index.php?title=Limiting-amplitude_principle&oldid=44712`. Accessed on 2020-05-4.

[5] M.-O. Bristeau, R. Glowinski, and J. Périaux. Controllability methods for the computation of time-periodic solutions; application to scattering. *Journal of Computational Physics*, 147(2):265–292, 1998.

[6] A. Brünger, C. L. Brooks III, and M. Karplus. Stochastic boundary conditions for molecular dynamics simulations of st2 water. *Chemical physics letters*, 105(5):495–500, 1984.

[7] H. Calandra, S. Gratton, X. Pinel, and X. Vasseur. An improved two-grid preconditioner for the solution of three-dimensional Helmholtz problems in heterogeneous media. *Numer. Linear Algebra Appl.*, 20(4):663–688, 2013.

[8] M. J. Gander and H. Zhang. A class of iterative solvers for the helmholtz equation: Factorizations, sweeping preconditioners, source transfer, single layer potentials, polarized traces, and optimized schwarz methods. *Siam Review*, 61(1):3–76, 2019.

[9] M. J. Grote, F. Nataf, J. H. Tang, and P.-H. Tournier. Parallel controllability methods for the helmholtz equation. *Computer Methods in Applied Mechanics and Engineering*, 362:112846, 2020.

[10] M. J. Grote and J. H. Tang. On controllability methods for the helmholtz equation. *Journal of Computational and Applied Mathematics*, 358:306–326, 2019.

[11] O. Holberg. Computational aspects of the choice of operator and sampling interval for numerical differentiation in large-scale simulation of wave phenomena. *Geophys. Prosp.*, 35(6):629–655, 1987.

[12] N. Kukreja, M. Louboutin, F. Vieira, F. Luporini, M. Lange, and G. Gorman. Devito: Automated fast finite difference computation. In *2016 Sixth International Workshop on Domain-Specific Languages and High-Level Frameworks for High Performance Computing (WOLFHPC)*, pages 11–19. IEEE, 2016.

[13] X. Liu, Y. Xi, Y. Saad, and M. V. de Hoop. Solving the 3d high-frequency helmholtz equation using contour integration and polynomial preconditioning. *arXiv preprint arXiv:1811.12378*, 2018.

[14] J. Poulson, B. Engquist, S. Li, and L. Ying. A parallel sweeping preconditioner for heterogeneous 3d helmholtz equations. *SIAM Journal on Scientific Computing*, 35(3):C194–C212, 2013.

[15] A. W. Sandvik. Numerical solutions of classical equations of motion. `http://physics.bu.edu/py502/lectures3/cmotion.pdf`. Lecture Notes Boston University PY 502, accessed: 2020-01-13.

[16] T. Schlick. *Molecular modeling and simulation: an interdisciplinary guide: an interdisciplinary guide*, volume 21. Springer Science & Business Media, 2010.

[17] C. C. Stolk. A dispersion minimizing scheme for the 3-d Helmholtz equation based on ray theory. *Journal of computational Physics*, 314:618–646, 2016.

[18] C. C. Stolk. An improved sweeping domain decomposition preconditioner for the Helmholtz equation. *Advances in Computational Mathematics*, 43(1):45–76, 2017.

[19] C. C. Stolk, M. Ahmed, and S. K. Bhowmik. A multigrid method for the Helmholtz equation with optimized coarse grid corrections. *SIAM Journal on Scientific Computing*, 36(6):A2819–A2841, 2014.

[20] G. Sutmann. Compact finite difference schemes of sixth order for the helmholtz equation. *Journal of Computational and Applied Mathematics*, 203(1):15–31, 2007.

[21] C. K. Tam and J. C. Webb. Dispersion-relation-preserving finite difference schemes for computational acoustics. *Journal of computational physics*, 107(2):262–281, 1993.

[22] M. Taus, L. Zepeda-Núñez, R. J. Hewett, and L. Demanet. L-sweeps: A scalable, parallel preconditioner for the high-frequency helmholtz equation. *arXiv preprint arXiv:1909.01467*, 2019.

[23] E. Turkel, D. Gordon, R. Gordon, and S. Tsynkov. Compact 2D and 3D sixth order schemes for the Helmholtz equation with variable wave number. *Journal of Computational Physics*, 232(1):272 – 287, 2013.

[24] S. Wang, M. V. De Hoop, and J. Xia. On 3d modeling of seismic wave propagation via a structured parallel multifrontal direct Helmholtz solver. *Geophys. Prospect*, 59:857–873, 2011.

[25] L. Zschiedrich, S. Burger, B. Kettner, and F. Schmidt. Advanced finite element method for nano-resonators. In *Physics and Simulation of Optoelectronic Devices XIV*, volume 6115, page 611515. International Society for Optics and Photonics, 2006.

Appendix A. Fourier analysis on $\Delta t \mathbb{Z}$

We consider the Fourier transform of functions on the grid $\Delta t \mathbb{Z}$. Let $g(n)$ be a function $\mathbb{Z}$. Considering n as a position variable, we have the following Fourier transform / inverse Fourier transform pair, denoting the frequency by ν

$$
\begin{aligned}
\widehat{g}(\nu) &= \sum_{n \in \mathbb{Z}} g(n) e^{-in\nu} \\
g(n) &= \frac{1}{2\pi} \int_{-\pi}^{\pi} \widehat{g}(\nu) e^{in\nu} \, d\nu.
\end{aligned}
$$

(111)

Here ν in the periodic interval $[-\pi, \pi]$ which we will also denote by $\mathbb{T}_{2\pi}$. We will also denote the Fourier transform of a function g by $\mathcal{F}g$.

For a function $f(t)$, $t \in \Delta t \mathbb{Z}$ it is convenient to generalize this as follows

$$\widehat{f}(\tau) = \Delta t \sum_{t \in \Delta t \mathbb{Z}} f(t) e^{-it\tau}.$$

(112)

$$f(t) = \frac{1}{2\pi} \int_{-\pi/\Delta t}^{\pi/\Delta t} \widehat{f}(\tau) e^{it\tau} \, d\tau.$$

For functions of $t \in \Delta t \mathbb{Z}$ the Dirac delta function will be defined by

(113)
$$\delta(t) = \begin{cases} \frac{1}{\Delta t} & \text{if } t = 0 \\ 0 & \text{otherwise} \end{cases}$$

It has Fourier transform

(114)
$$\mathcal{F}\delta(\tau) = 1.$$

For function $g(t), h(t)$, $t \in \Delta\mathbb{Z}$, we have

(115)
$$\widehat{gh} = \frac{1}{2\pi}\widehat{g} * \widehat{h}$$

where $*$ denotes convolution on $\mathbb{T}_{2\pi/\Delta t}$.

Appendix B. Additional material for subsection 3.2

In case of variable coefficients, the 27 point optimized finite-differences discretization used in subsection 3.2 is done in a quasi-finite-element way that we now explain. This is consistent with [17].

We first define some notation. In this appendix, three dimensional indices are denoted by greek letters, e.g. $\alpha = (\alpha_1, \alpha_2, \alpha_3)$. A grid cell will have the same index as the point in the lower (in all dimensions) corner. The set of corners of a grid cell will be denoted by $C(\alpha)$. We define

(116)
$$\Delta(\alpha, \beta) = |\alpha_1 - \beta_1| + |\alpha_2 - \beta_2| + |\alpha_3 - \beta_3|.$$

If α, β are two corner points of a grid cell, then this number is 0 if they are the same and 1, 2, or 3 if they are opposite points on an edge, face, or the cell itself respectively. We define

(117)
$$\tilde{f}_s\left(\frac{kh}{2\pi}\right) = \frac{1}{2^{3-s}} f_s\left(\frac{kh}{2\pi}\right)$$

In case of variable coefficients, the coefficient k will be constant on grid cells, its value is denoted by $k^{(\alpha)}$

The matrix $\mathrm{Re}\, H$ will be associated with a bilinear form

(118)
$$\mathcal{H}(v, u) = \sum_{\text{cells } \alpha} \mathcal{H}_{\text{cell}}(\alpha; v, u).$$

The contribution for a single cell is given by

(119)
$$\mathcal{H}_{\text{cell}}(\alpha; v, u) = \sum_{\beta, \gamma \in C(\alpha)} \tilde{f}_{\Delta(\beta,\gamma)}\left(\frac{hk^{(\alpha)}}{2\pi}\right) v^{(\beta)} u^{(\gamma)}$$

For each cell we have

(120)
$$\mathcal{H}_{\text{cell}}(\alpha; u, u) \geq -(k^{(\alpha)})^2 \frac{1}{8} \sum_{\beta \in C(\alpha)} \left|u^{(\beta)}\right|^2.$$

An expression for $\lambda_{\min}(\mathrm{Re}\, H)$ follows straightforwardly from this. For an upperbound for $\lambda_{\max}(\mathrm{Re}\, H)$ one can use (70) with k replaced by $k_{\min}$.